APOLLO 15 AND 16 RESULTS OF THE INTEGRATED GEOCHEMICAL EXPERIMENT*

I. ADLER, J. I. TROMBKA, P. LOWMAN, R. SCHMADEBECK, H. BLODGET, E. ELLER, L. YIN, R. LAMOTHE, and G. OSSWALD
NASA/Goddard Space Flight Center, Greenbelt, Md., U.S.A.

J. GERARD
Eastman Kodak Research Labs, Rochester, N.Y., U.S.A.

P. GORENSTEIN, P. BJORKHOLM, H. GURSKY, and B. HARRIS
American Science and Engineering, U.S.A.

J. ARNOLD
University of California, San Diego, Calif., U.S.A.

A. METZGER
Jet Propulsion Laboratory, Pasadena, Calif., U.S.A.

and

R. REEDY
Los Alamos Scientific Lab., Los Alamos, N.M., U.S.A.

(Received 4 December, 1972)

Abstract' A number of experiments carried in orbit on the Apollo 15 and 16 spacecraft were used in the compositional mapping of the lunar surface. The observations involved measurements of secondary (fluorescent) X-rays, gamma rays and alpha particle emissions. A large scale compositional map of over 20% of the lunar surface was obtained for the first time. It was possible to demonstrate significant chemical differences between the mare and the highlands, to find specific areas of high radioactivity and to learn something about the composition of the Moon's hidden side.

1. Introduction

The earliest American effort at remote analysis of the Moon dates back to the attempt at gamma ray spectroscopy during the Ranger 3, 4 and 5 flyby flights (Van Dilla *et al.*, 1962). Gamma ray experiments were also carried aboard the Russian Luna 10 and 11, vehicles placed in orbit around the Moon (Vinogradov *et al.*, 1968). The first approach to measuring fluorescent X-rays from the lunar surface was made on the orbiting Luna 12 by Mandel'shtam and co-workers (1968). Although few compositional data were obtained there were positive indications that the sun does produce measureable fluorescent X-rays from the lunar surface. The concept of flying an integrated geochemical package for the remote analysis of the lunar surface was discussed in a report issued as a result of a Goddard Space Flight Center study (Carpenter *et al.*, 1968). It was pointed out that the absence of a lunar atmosphere would permit the use of an orbiting vehicle for widespread observations of the lunar

* Paper dedicated to Professor Harold C. Urey on the occasion of his 80th birthday on 29 April 1973.

The Moon 7 (1973) 487–504.

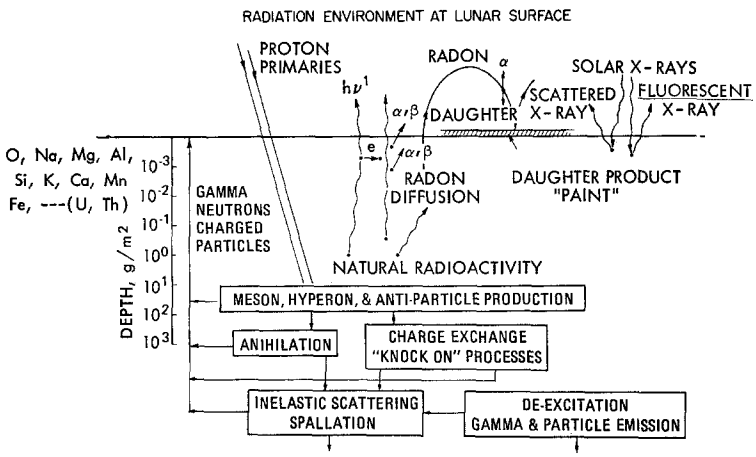

Fig. 1. The radition environment at the lunar surface.

surface by simultaneous measurements of certain non-optical electromagnetic radiation as well as charged particles. Figure 1 is a summary of our view of the radiation environment at the Moon's surface. The report considered the possible sources of geochemical information produced by the various interactions occuring at the lunar surface and near lunar surface. A number of orbital experiments were proposed to utilize these interactions in producing a large scale geochemical map.

As we see both natural and induced sources of radiation are present. Among the naturally occurring radioactive constituents are the long lived nuclides ^{40}K, ^{238}U, ^{232}Th and their decay products. These are sources ot alpha, beta and gamma radiation of various energies. Special processes such as radon diffusion (Kraner *et al.*, 1966) may also occur. Bombardment of the lunar surface by cosmic rays and energetic solar protons also produces a variety of shorter lived nuclides and thus induced activity as well as a prompt emission of charged particles, neutrons and photons.

Solar X-rays absorbed in the lunar surface produce fluorescent X-rays characteristic of some of the chemical elements in the surface. The relative yields of the secondary X-rays depends on the intensity and spectral character of the solar X-ray flux as well as the relative abundance of the elements. Figure 1 also shows that if radon and thoron diffusion through the surface occurs, they would be expected to produce alpha particles characteristic of the various decay processes. Using the above as a basis and governed by spacecraft limitations, experiment packages consisting of gamma ray, X-ray and alpha particle spectrometers were proposed and then flown during the Apollo 15 and 16 missions. The basic theory and the experiments will be briefly described below.

2. Gamma Ray Experiment

Gamma rays are either absorbed or scattered in the lunar soil or rock in a layer of the order of tens of centimeters. Thus a device which measures gamma rays is sampling

the composition of the Moon to depths of this order. Because such a depth is well within the regolith layer one can assume it to be fairly well mixed.

The chemical information contained in a gamma ray spectrum is found in discrete lines with characteristic energies (Reedy *et al.*, 1972). These lines fall into two groups, one from the decay of the naturally occurring radioactive elements ^{40}K and the radioactive daughters of Th and U. Examples are the 1.46 MeV line from ^{40}K decaying to ^{40}Ar and the 2.62 MeV line of ^{208}Tl (daughter of ^{232}Th). A second group of lines results from the bombardment of the lunar surface by high-energy charged particles, the cosmic rays. These cosmic rays, essentially of galactic origin, interact to produce a cascade of lower energy particles of which the most important are neutrons. These neutrons in turn produce excited nucleii which emit radiation in three ways; inelastic scatter, neutron capture and nuclear reactions. Inelastic scattering is an important process for neutron energies of a few MeV and one can expect discrete lines from each of the major elements, for example the 0.84 MeV line of Fe. In the second major process, neutron capture, neutrons lose energy by successive collisions, until those that do not excape through the surface are captured. The binding energy of the added neutron, typically about 8 MeV is emitted from the compound nucleus in a complex decay scheme, which occasionally results in dicrete lines, for example an Fe line at 7.64 MeV. The third process, involving nuclear reactions is generally less important. Gamma rays are emitted by the radioactive nuclides produced by nuclear reactions an example of which is ^{26}Al from Al by $(n, 2n)$ and Si by $(n, 2np)$.

Finally the Sun may also be a source of energetic particles which produce gamma ray or radioactive nucleii in the Moon during major solar flares. This follows from the interaction of solar cosmic rays with the lunar surface. The particles in the energy range of 10–100 MeV lose energy mainly by ionization and sometimes nuclear reactions.

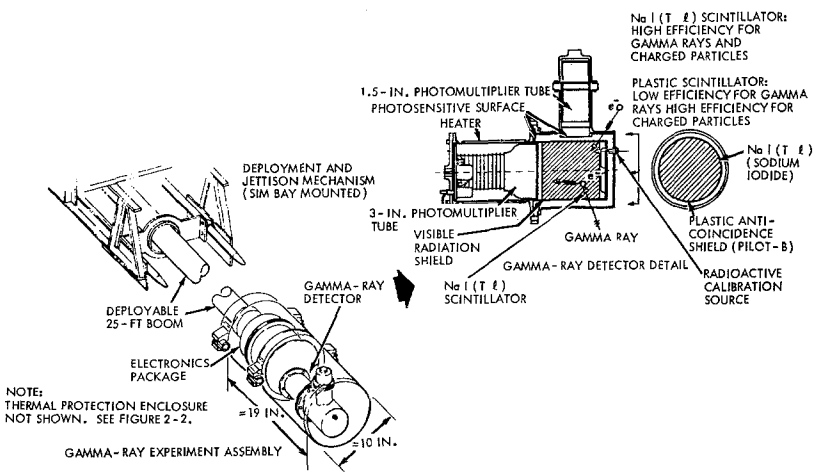

Fig. 2. Gamma-ray detector detail.

The intensities of the spectrum lines can be calculated as a function of the chemical composition, from a knowledge of the physical processes involved. In the case of the natural radioactivities, the calculations are simple and unambiguous. For the lines induced by high energy bombardment, the required fluxes and cross sections are known only approximately. Thus the availability of results (from returned lunar samples) for areas such as Mare Tranquillitatis and the Apollo 15 landing site is of great value.

The gamma ray instrument has been described in detail elsewhere. The incident gamma ray flux was sensed by a 7×7 cm, cylindrical sodium iodide scintillation detector and the out signal subjected to pulse height analysis (Arnold *et al.*, 1972). A sketch of the instrument is shown in Figure 2. A noteworthy feature of the experiment is that the Apollo 15 and 16 gamma ray detectors were operated at the end of a retractable boom, thus decreasing the response of the instrument to cosmic ray interactions and radioactive sources in the spacecraft.

3. X-Ray Fluorescence Experiment

From numerous calculations it was shown that the typical 'quiet' solar X-ray spectrum was energetically capable of producing measureable amounts of characteristic X-rays from all the abundant elements with atomic numbers of approximately 14 (Si) or smaller. During brief periods of more intense solar activity it was expected that characteristic X-rays from higher atomic number elements would also appear.

The quiet Sun solar X-ray flux has been studied at some length. The spectral distribution is known to decrease very sharply with increasing X-ray energies. If a strictly thermal mechanism of production is assumed, variable coronal temperatures are calculated which range between 10^6 and 10^7 K. Variations in temperature produce changes in flux and spectral composition. From our knowledge of the process of X-ray fluorescence production we can therefore expect a variation in X-ray fluorescent intensities and also in the relative intensities from the various chemical elements of the lunar surface. For example, a hardening of the solar spectrum would produce an enhancement of the heavier elements relative to the lighter ones.

A simplified estimate of the solar X-ray flux based on satellite data is shown in Figure 3. This results from combining the output of a 1.5×10^6 K corona with that from the more active regions at 3×10^6 K; the proportions determined by the satellite data and using the model developed by Tucker and Koren (1971). Superimposed on this curve along the energy axis are the K shell absorption edges for Na, Mg, Si and S. Only the solar X-rays with energies on the high side of the absorption edges are capable of exicting these elements, and to a degree depending on the incident flux and the ionization cross sections. Thus, under quiet Sun conditions, the solar flux is most suitable for exciting the light elements, including the major rock forming elements Si, Al and Mg. Although these are only a small proportion of the number of interesting elements they nevertheless represent very important diagnostic element in studying the Moon's evolution.

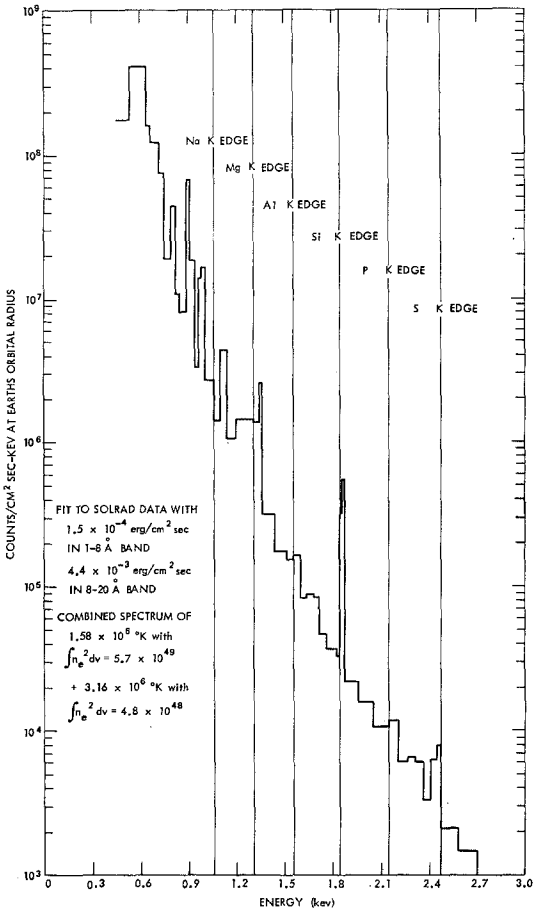

Fig. 3. A simplified estimate of emitted solar X-ray flux based on satellite data and model developed by Tucker and Thoren (1971).

A diagram of the functional configuration of the X-ray spectrometer is shown in Figure 4. The experiment has been described in detail in a previous report (Adler *et al.*, 1972). Essentially the spectrometer depends on energy sensitive detectors (proportional counters), selective X-ray filters and pulse height analysis. Because of the variable nature of the solar X-ray flux a small proportional counter on the opposite side of the spacecraft was used to monitor the Sun throughout the mission. The nature of the detector configuration provided a nominal 60° field of view. At the mission altitude of nearly 110 km this permitted an instantaneous sample area approximately 100 km on edge.

4. Alpha Particle Experiment

Of the various phenomena involving alpha particle emission from the lunar surface, the most interesting from a geochemical point of view is the production of alpha

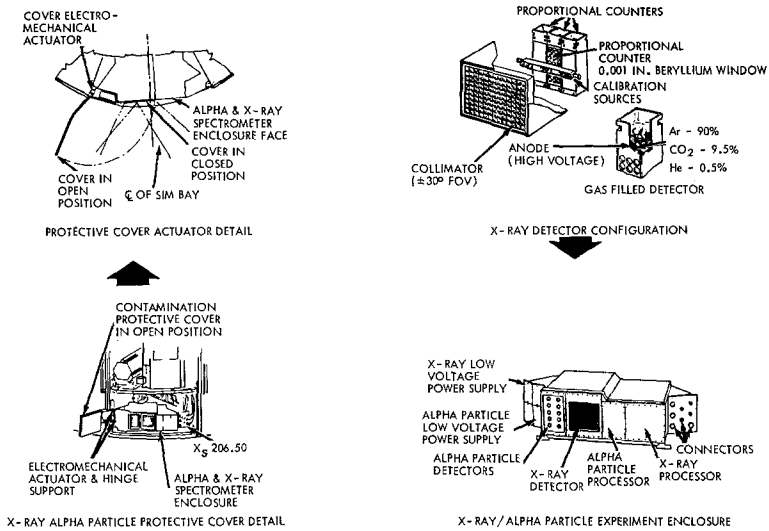

Fig. 4. A functional configuration of the X-ray fluorescence spectrometer.

particles due to the possible diffusion of radon (^{222}Rn) and thoron (^{220}Rn) through the lunar surface. In the mechanism proposed by Kraner *et al.*, (1966), the radon and and thoron produce a 'paint' on the surface made up of the decay products. If thermal velocities are assumed for the emerging radon and thoron, then nearly all the molecules would be trapped in the Moon's gravitational field. Radon with a 3.8 day half life would be expected to travel a considerable distance before undergoing decay, Thoron on the other hand, with a 55 s half life would be expected to decay near its source. Both of these species would yield daughter products giving characteristic spectral lines. The equipment for alpha particle measurements is shown in Figure 5. The detectors are solid state surface barrier types. The total experimental arrangement involved 10 distinct detectors mounted in the same package as the X-ray spectrometer.

5. Results of the Orbital Geochemistry Measurements

The sections below summarize the results obtained with the integrated geochemistry experiment for both the Apollo 15 and 16 flights. The Apollo 15 to Hadley Rille

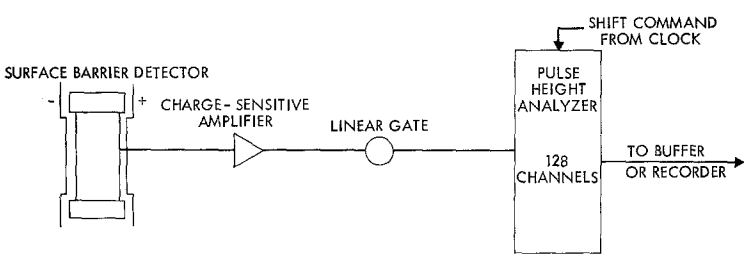

Fig. 5. Alpha particle detector.

was at an orbital inclination of 26 while the Apollo 16 to Descartes flew at about 9°. As a consequence, the Apollo 15 ground track covered a larger projected area than the Apollo 16. Because the fluorescent X-rays are produced by the Sun, the observations covered only that part of the moon illuminated by the Sun. Further the results obtained near both terminators were less reliable because of poorer statistics. By contrast the gamma ray and alpha particle measurements covered a band completely around the Moon. There was some overlap of coverage between Apollo 15 and 16 missions (see Figure 6) which permitted a comparison of the results from both flights.

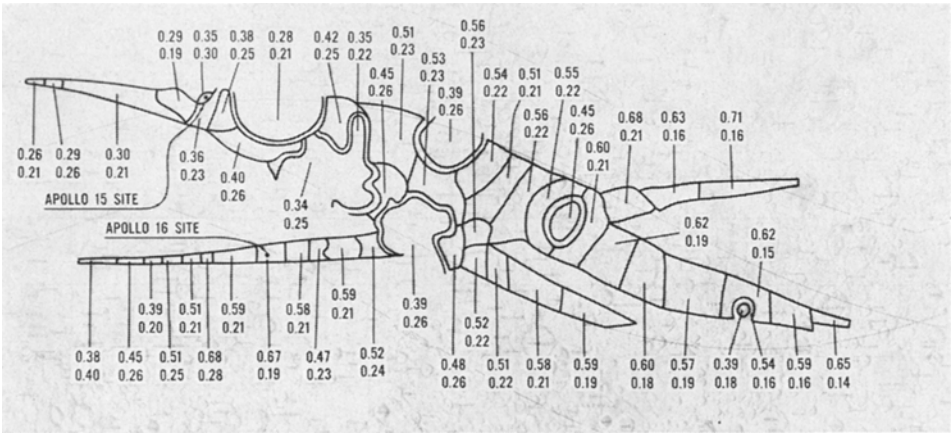

Fig. 6. Variation of Al/Si and Mg/Si concentration ratios along the projected ground tracks for Apollo 15 (upper envelope) and Apollo 16 (lower envelope). The upper values in each square correspond to Al/Si and the lower numbers to Mg/Si.

The X-ray fluorescence results were reproducible enough for both missions so that no normalization was required. The Apollo 15 flight coved such areas as the craters Gagarin, Tsiolkovsky, the far side and eastern limb highlands, the maria such as Smythii, Crisium, Fecunditatis, Tranquillitatis, Serenitatis, Imbrium, Oceanus Procellarum, the Haemus Mountains and the Apennines. To this Apollo 16 added Mare Cognitum, Mare Nubium, Ptolemaeus, the Descartes region and Mendeleev.

The X-ray fluorescence experiment performed very well during both flights so that over 100 h of data were obtained during Apollo 15 and at least 60 h during Apollo 16. The Sun proved to be relatively stable during both missions except for a few brief periods of increased activity. These periods were readily identified in our solar monitor data.

The methods of data reduction of the X-ray data have been described in detail elsewhere (Adler *et al.*, 1972). The data were reduced to Al/Si and Mg/Si in tensity ratios and then finally to chemical ratios.

Figure 6 shows the Al/Si and Mg/Si concentration ratios along the projected ground tracks for Apollo 15 (upper envelope and Apollo 16 (lower envelope)). These values are shown in relation to some of the major featurs. This relationship

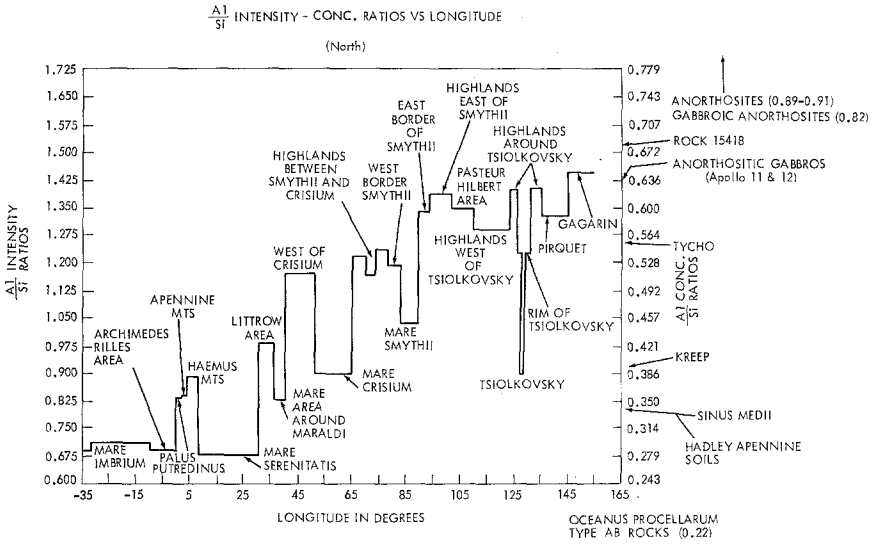

Fig. 7a. Al/Si ratios vs. longitude for the Apollo 15 ground track. The values for some reference materials are shown on the vertical axis.

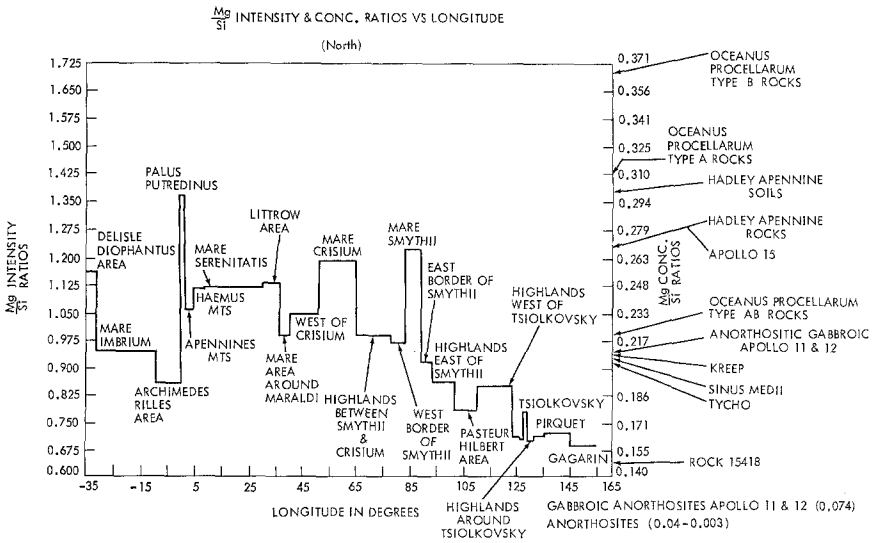

Fig. 7b. Mg/Si ratios for the same tracks as above.

is shown in greater detail for Al/Si and Mg/Si in Figures 7 (a and b) and 8 (a and b) for both missions. The ratios for various analyzed materials are shown along the right hand axis for reference. A summary of representative ratios for both missions is given in Table I. Table II shows the agreement between both missions for the overlap regions.

A number of observations have been drawn from the data:

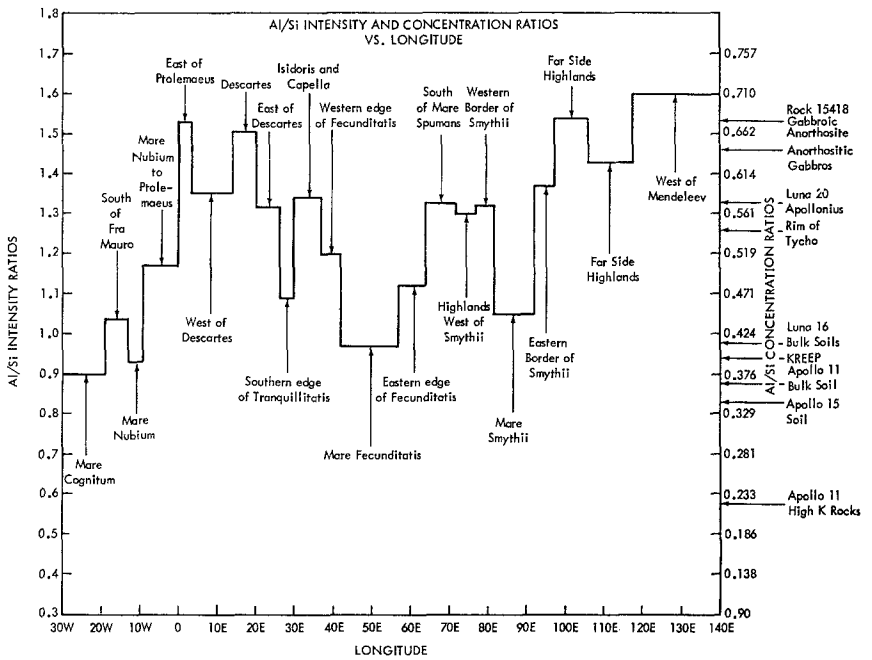

Fig. 8a. Al/Si ratios for the Apollo 16 ground track.

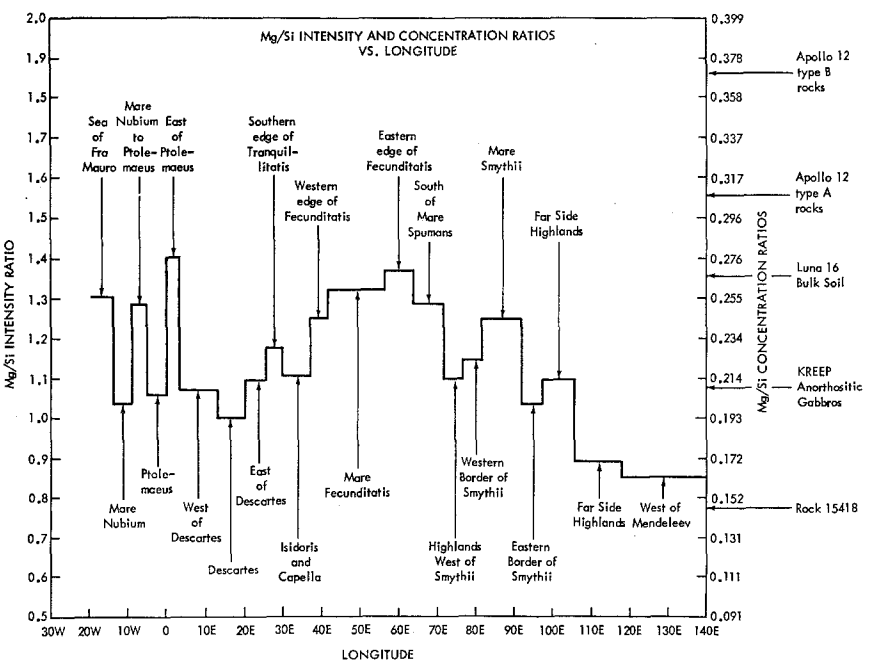

Fig. 8b. Mg/Si ratios for the same track.

TABLE I

Concentration ratios of Al/Si and Mg/Si for various features

Feature	N [a]	Concentration ratios	
		Al/Si $\pm 1\sigma$	Mg/Si $\pm 1\sigma$
Mare Cognitum	8	0.38 ± 0.11	0.40 ± 0.29
Upper part of Sea of Clouds (9°–13° W)	8	0.39 ± 0.12	0.20 ± 0.05
Mare Fecunditatis (42°–57° E)	80	0.41 ± 0.05	0.26 ± 0.05
South of Fra Mauro (13°–19° W)	9	0.45 ± 0.07	0.26 ± 0.04
Mare Smythii (82°–92° E)	24	0.45 ± 0.08	0.25 ± 0.04
Southern edge of Mare Tranquillitatis, Torricelli area (26°–30° E)	21	0.47 ± 0.09	0.23 ± 0.05
Eastern edge of Fecunditatis, Langrenus area (57°–64° E)	44	0.48 ± 0.07	0.27 ± 0.06
Ptolemaeus (4° W–0.5° E)	17	0.51 ± 0.07	0.21 ± 0.04
Highlands west of Ptolemaeus to Mare Nubium (4°–9° W)	16	0.51 ± 0.11	0.25 ± 0.12
Highlands west of Mare Fecunditatis (37.5°–42° E)	29	0.52 ± 0.07	0.24 ± 0.05
Highlands west of Smythii (72°–77° E)	35	0.57 ± 0.07	0.21 ± 0.03
Western border of Smythii (77°–82° E)	33	0.58 ± 0.08	0.22 ± 0.04
Highlands east of Descartes (20.5°–26° E)	23	0.58 ± 0.07	0.21 ± 0.04
South of Mare Spumans (64°–72° E)	45	0.58 ± 0.07	0.25 ± 0.04
Isidorus and Capella (3°–37.5° E)	38	0.59 ± 0.11	$0.21 \pm .$
Highlands west of Descartes (3°–14° E)	44	0.59 ± 0.11	0.21 ± 0.05
Eastern border of Mare Smythii (92.5°–97.5° E)	17	0.61 ± 0.09	0.20 ± 0.06
Far-side highlands (106°–118° E)	29	0.63 ± 0.08	0.16 ± 0.05
Descartes area, highlands, Apollo 16 landing site (14°–20.5° E)	30	0.67 ± 0.11	0.19 ± 0.05
East of Ptolemaeus (0.5°–3° E)	12	0.68 ± 0.14	0.28 ± 0.09
Highlands (97.5°–106° E)	31	0.68 ± 0.11	0.21 ± 0.05
Far-side highlands west of Mendeleev (118°–141° E)	30	0.71 ± 0.11	0.16 ± 0.04

[a] N is the number of individual data points used to determine the average Al/Si and Mg/Si values $\pm$ 1 standard deviation and was obtained from the various passes over each feature.

TABLE II

Overlap between the Apollo 15 and 16 ground tracks

Feature[a]	Apollo 16 concentration ratio		Apollo 15 concentration ratio	
	Al/Si $\pm 1\sigma$	Mg/Si $\pm 1\sigma$	Al/Si $\pm 1\sigma$	Mg/Si $\pm 1\sigma$
Mare Fecunditatis	0.41 ± 0.05	0.26 ± 0.05	0.36 ± 0.06	0.25 ± 0.03
Mare Smythii	0.45 ± 0.08	0.25 ± 0.05	0.45 ± 0.06	0.27 ± 0.06
Langrenus area	0.48 ± 0.07	0.27 ± 0.06	0.48 ± 0.11	0.24 ± 0.06
Highlands west of Smythii	0.57 ± 0.07	0.21 ± 0.03	0.55 ± 0.06	0.22 ± 0.03
Western border of Smythii	0.58 ± 0.08	0.22 ± 0.04	0.52 ± 0.06	0.22 ± 0.06
Eastern border of Smythii	0.61 ± 0.09	0.20 ± 0.06	0.60 ± 0.10	0.21 ± 0.03

[a] The overlap between corresponding areas of the Apollo 16 and 15 ground tracks is not exact, so that differences for the same area may real (Figure 19-2).

(1) The Al/Si ratios are highest in the eastern limb highlands and considerably lower in the mare areas. The extreme variation is about a factor of two; the lowest value occurring in the Imbrium basin region. The Mg/Si concentration ratios generally show the opposite relationship. The Al/Si and Mg/Si chemical ratios for the highlands correspond to that for anorthositic gabbro through gabbroic anorthosites or feldspathic basalts. By contrast the chemical ratios for the mare areas correspond to the mare basalts.

(2) Our early reports, while Apollo 16 was in progress, of very high Al/Si ratios in the Descartes area have been confirmed by the analysis of the returned lunar samples from the site. The values reported of 26.5% aluminum oxide agree very well with our own estimates (see Table II). It appears reasonable from the data that some of the material sampled at Descartes is similar to that of the eastern limb and far side highlands. This conclusion is further justified by the fact that the Mg/Si concentration ratios for some of the returned materials is about 0.18, close to our reported values of 0.19 ± 0.05. The eastern limb highlands and far side highlands as shown in Table I are about 0.16–0.21.

(3) In both missions the Al and Mg values for most part show an inverse relationship.

(4) There are distinct chemical contrasts between such features as the small mare basins and the highland rims (note for example the crater Tsiolkovsky in Figure 7).

An interesting use of the data has involved a comparison of Al/Si intensity ratios versus optical albedo values. These observations are particularly significant in view of the longstanding discussions about whether these albedo differences are solely representative of topographic differences or also a reflection of compositional differences among surface materials. Early workers such as Whitaker (1965) and others had recognized convincing evidence for compositional changes where sharp albedo changes occur. However, it remained for the later Surveyor, Apollo, Luna and Lunakhod missions to provide quantitative compositional data. Chemical differences related to albedo variations were first confirmed by the Alpha Backscattering Experiment carried on Surveyors 5, 6, and 7 (Patterson, 1972). Surveyors 5 and 6 analyzed widely separated mare sites and reported chemically similar surface materials in each. Surveyor 7 on the other hand, analyzed a highland site and found a significant chemical difference between it and the two mare locations. The Surveyor results and the analyses of returned lunar samples confirmed that the albedo is indeed affected by composition as well as topographic differences. The X-ray Fluorescence experiment on Apollo 15 and 16 now has provided the means to correlate regional albedo with surface composition (for selected chemical elements).

The data from both Apollo flights showed an excellent correspondence between Al/Si values and the optical albedo values. An example from the Apollo 16 flight is shown in Figure 9. There is positive correlation between the albedo and the Al/Si values although the rate of change is not always similar. In the Apollo 15 plots the main anomalies were observed where an occasional small Copernican type crater occurred, and produced an abnormally high albedo value. This was considered to be due to the highly-reflective, finely divided ejecta rather than to compositional

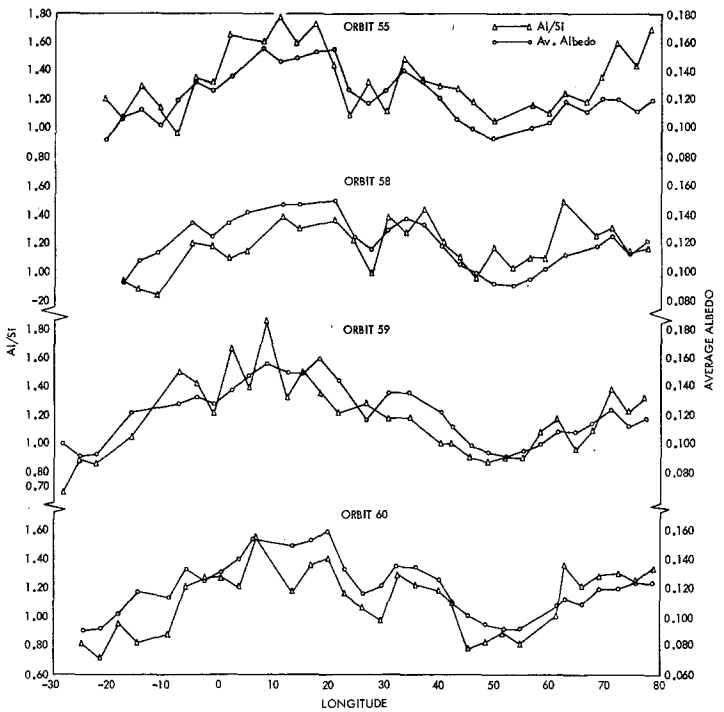

Fig. 9. A comparison of Al/Si intensity ratios vs. optical albedo values for various Apollo 16 orbits.

changes. A similar anomaly is noted in the Apollo 16 data around 27° west longitude in a Tranquillitatis embayment north of Theophilus. Four Apollo 16 orbits are plotted. Orbits 58 and 60 show the expected decrease in Al/Si with decreasing albedo. Orbits 55 and 59 on the other hand, show an occasional increase in Al/Si although the albedo decreases. This may record the existence of an old 'weathered' ray consisting of aluminum rich highland derived ray material which has lost its high reflectivity.

6. Gamma Ray Results

Like the X-ray fluorescence experiment the gamma ray experiment also performed very well during both missions. The Apollo 16 instrumentation was improved over the Apollo 15 device several ways. The energy resolution of the spectrometer was improved from about 8.5% to 7.5% leading to better line resolution and precision; there was reduced gain drift, an increase in the amount of prime data and finally a much more rapid reduction of data during the course of the mission.

The spectrometers flown were essentially isotropic in look angle. The field of view was defined by the orbit which for both missions was nearly circular with a mean altitude of 110 km. Thus about one half of the lunar photons reaching the detector originated inside a circle of about 120 km from the subspacecraft point. Telemetry

did not limit the field of view because the data was transmitted or recorded on an event by event basis.

A typical gamma ray spectrum taken from Apollo 15 for seven hours of operation over the trajectory is shown in Figure 10. As was expected the flux decreases rapidly with increasing energy and the continuum dominates over the line structure. It is possible to identify some characteristic line features attributable to both natural radioactivity and induced emission. The natural species are K, Th and U while the inelastic prompt gamma lines are Fe, Mg, Si and O. These lines stand out much more clearly when an estimated continuum contribution is subtracted leaving a net pulse height spectrum as shown in the figure.

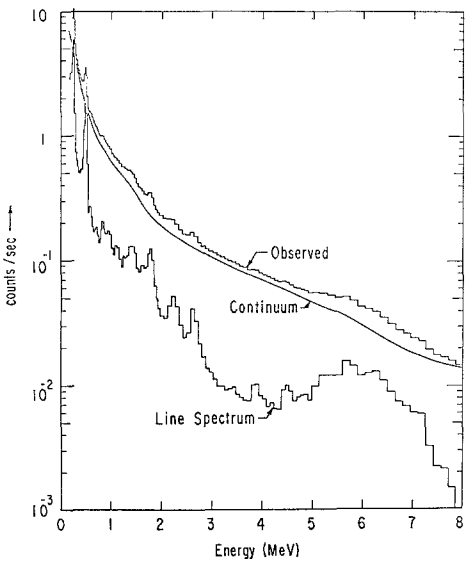

Fig. 10. A typical gamma-ray spectrum taken from Apollo 15. The spectrum is dominated by continuum. The observed spectrum with continuum subtracted is also shown. The characteristic lines are now much more evident.

Variations in lunar surface composition were observed by accumulating the events in various energy intervals for increments of lunar surface area. A very useful energy interval is the range of 0.55–2.75 MeV because it contains the major lines due to the decay of K, U, and Th as well as their daughter products. This region also includes a large proportion of the Compton scattering and pair production interactions which deposit only a portion of their energy in the detector. The observed spatial distribution of natural radioactivity during the Apollo 15 and 16 experiments for the nearside and farside faces of the Moon was examined (see Figure 11). The natural radioactivity was found to be concentrated in the Mare Imbrium-Oceanus Procellarum region. Within this region three highs were observed, one around Aristarchus, a second in the southeastern region of Mare Imbrium and the third south of Fro Mauro. The level

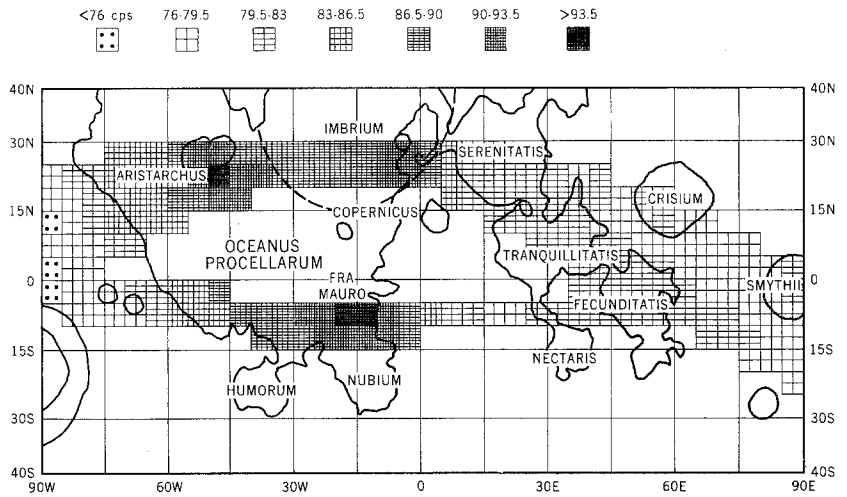

Fig. 11. Apollo 15 and 16 longitudinal regional accumulation of radioactivity.

of radioactivity falls off rapidly as one crosses into the highlands area west of Oceanus Procellarum. The highlands everywhere else are almost uniformly at the low concentration end of the scale. The one notable exception is near the farside crater Van de Graff where interestingly enough in addition to the pronounced increase in radioactivity the sub-satellite has reported a large magnetic anomaly and the flight laser altimeter a major depression (Coleman, 1972; Kaula, 1972).

7. Results of the Alpha Particle Experiment

Although data taken during the Apollo 15 and 16 flights show that the observed alpha activity was very small, of the order of 10^{-3} counts cm^{-2} s^{-1}. positive results were obtained relating to the distribution of radon and her daughter products. Three distinct types of signals were sought: alpha particles having energies consistent with the decay of ^{222}Rn and the daughter products, alpha particles from ^{220}Rn and the daughter products and finally alphas from ^{210}Po. The first two are associated with current activity and the last with events having occurred days to years previously (the presence of ^{210}Po is determined by the decay of ^{210}Pb with its 22-yr half life).

In searching for evidence of the ^{222}Rn two methods were used in processing the data. The first method involved a comparison of the counts obtained in the appropriate energy channels with the detectors looking at the lunar surface and then away. The second method involved examining the total energy spectrum and looking for an increase in those energy channels where the alphas from the ^{222}Rn were expected to occur.

An additional step in the analysis was to see if enhanced signals could be-attributed to any localized area. This was done by producing a crude map of alpha-activity

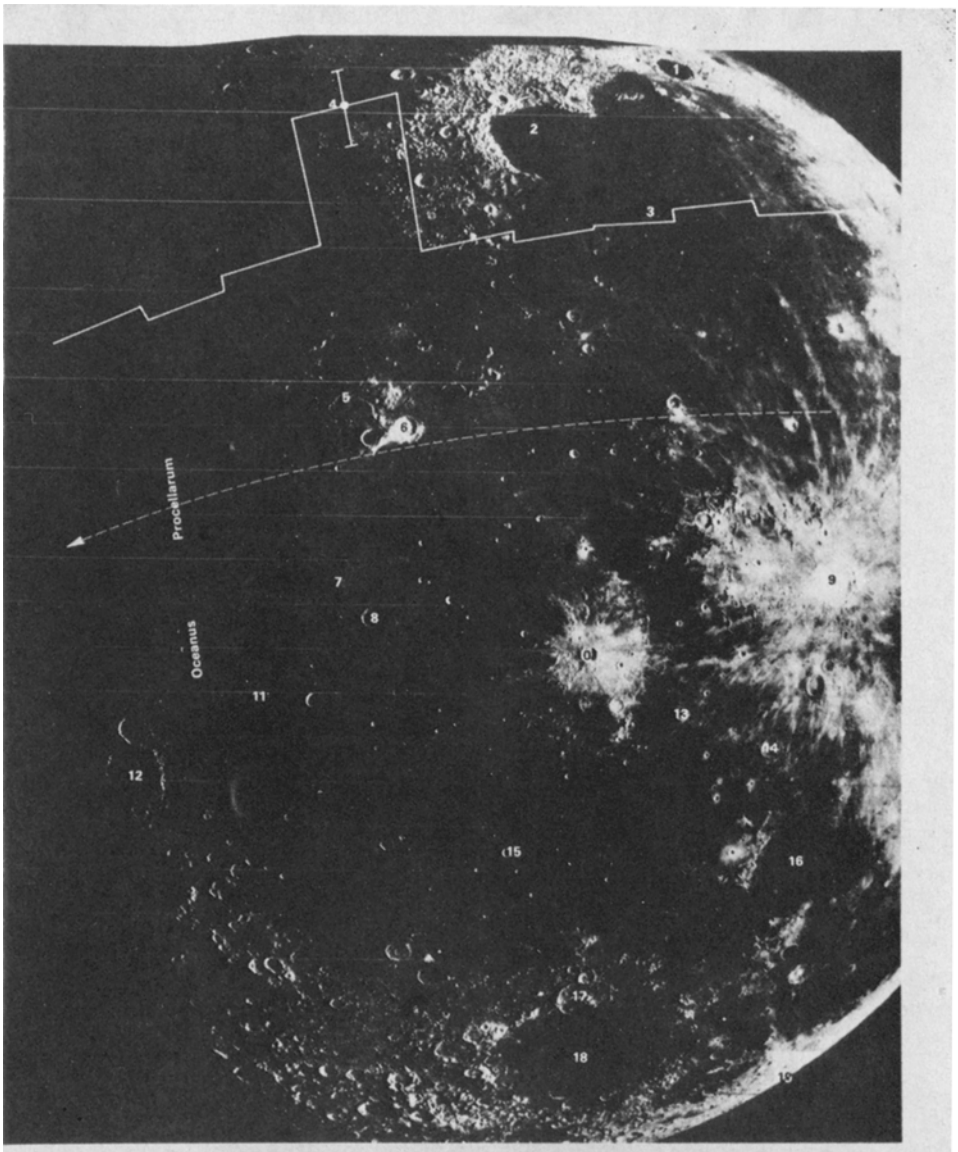

Fig. 12. The variation or ^{222}Rn superimposed upon a photograph of the Moon. The dashed line represents the average ground track during Apollo 15 orbits 34–36. It is also the baseline for the data.

over the ground tracks, dividing the data into bins approximately 5° in longitude and variable latitudes (less than 12°). Two features were obvious from the Apollo 15 data. The first feature occurs between 45° and 50° west and only where the crater Aristarchus is within the instruments field of view. Figure 12 shows the count rate for decays from ^{222}Rn and daughter products (excluding ^{210}Po). The dashed line is the approximate ground track during the period of data collection (revs. 36–46). The count rate over Aristarchus exceeds the mean count rate for the whole Moon by 4.3 standard deviations. There is also an indication of a general increase in count rate over Oceanus Procellarum and Mare Imbrium which is under further study.

The results from Apollo 16 are still preliminary and obtained from some of the 'quick look' data obtained while the mission was in progress. The most striking result is the strong evidence for the existence of decays from ^{210}Po, indicated by a statistically significant higher count rate centered over the Mare Fecunditatis. There are also indications of another concentration of ^{222}Rn like feature detected in the vicinity of Aristarchus from Apollo 15.

The conclusions drawn from the Alpha experiment on Apollo 15 and 16 is that there are areas on the Moon with locally high emanations. The most conspicuous feature is in the region which includes the crater Aristarchus. The enhanced activity may be an indication of internal activity at the site. The existence of regions showing some ^{210}Po activity is perhaps an instance of some previous, transient phenomenon involving the release of ^{222}Rn from some area of the Moon.

8. Geologic Interpretation of Orbital Experimental Results

The Apollo 16 results generally support the conclusions reached after the Apollo 15 mission (Adler *et al.*, 1972). The results when viewed in light of other evidence, give us a better understanding of the lithology of the Moon's highland crust, and by implication, its petrologic evolution. One of the most important aspects of the geochemical measurements is that they give a good indication of how representative the returned samples are of the lunar surface in general. The excellent agreement between the Al_2O_3 and Th–U content of the returned Apollo 16 soil samples and that inferred from the X-ray and gamma ray measurements respectively demonstrate that the orbital measurements are a reliable guide to at least this aspect of the Moon's chemistry. As we have demonstrated the X-ray results also show that the optical albedo is a reasonable guide to the highland crustal composition.

The two ratios, Al/Si and Mg/Si do not uniquely specify any particular rock type. They do put limits on the constituents of the exposed crust; in particular anorthosite (pure plagioclase) is ruled out as the only constituent of the highlands. Since anorthosite plays a central role in several theories of lunar evolution (Wood, 1972), the demonstration that the highlands are only in part anorthosite is worth noting. The petrography of returned lunar highland samples (from the Apennine front at Hadley) suggests that the Mg/Si ratios are the expression of a pyroxene-bearing rock, such as 'norite' (Wood, 1972) or KREEP (Meyers *et al.*, 1972) which

is high in radioactivity and other trace elements and low in Al. Our own evidence (Adler *et al.*, 1972) however is that the Al/Si ratios of this rock type (about 0.4) are too low to account for the X-ray data over the highlands (0.5–0.65). Furthermore, the gamma ray measurements from Apollo 15 and 16 (Arnold *et al.*, 1972) indicate too low a level of radioactivity in the highlands for KREEP. The gamma ray measurements also rule out large quantities of granite or its chemical equivalent for the highlands.

The widespread occurrence of plagioclase in returned highland and exotic mare materials, the Al/Si ratios and the positive correlation between optical albedo and the X-ray data show clearly that the highlands are dominatly feldspatic. A plagioclase-pyroxene-bearing rock is clearly indicated, corresponding to anorthositic gabbro or feldspathic basalt. Such rocks could form from magmas of their own composition, unlike the lunar anorthosites (Stewart *et al.*, 1972) and hence present no major petrologic difficulties. These magmas could produce anorthosite like rock 15425 by fractional crystallization.

This interpretation may indicate either differentiation of the Moon by generation of aluminum rich magma or enrichment of the outer layers in refractory elements such as calcium and aluminum (Hubbard and Gast, 1971) by alkali volatilization, or both. In any event, the X-ray measurements covering over 230 degrees of longitude, suggest that this crust originally covered the entire Moon (before excavation of the mare basins and eruption of the mare basalts). Based on results of the gamma ray experiment, the KREEP component appears to have originated in and be mainly confined to the western maria and their neighborhood. We are seeing on the Moon, therefore, evidence of some form of planetary differentiation that produced both a global and a local crust. This evidence may have implications for the evolution of the Earth and terrestrial planets as well as the Moon.

References

Adler, I., Trombka, J., Gerard, J., Schmadebeck, R., Lowman, P., Blodget, H., Yin, L., Eller, E., Lamothe, R., Gorenstein, P., Bjorkholm, P., Harris, B., and Gursky, H.: 1972, Preliminary Science Report; NASA-SP 289.

Arnold, J. R., Peterson, L. E., Metgzer, A. E., and Trombka, J. I.: 1972, Preliminary Science Report, NASA-SP 289.

Carpenter, J., Gorenstein, P., Gursky, H., Harris, B., Jordan, J., McCallum, T., Ortmann, M., and Sodickson, L.: 1968, Final Report-Lunar Surface Exploration by Satellite, NAS-11086.

Coleman, P. J., Jr., Russel, C. T., Sharp, L. R., and Schubert, G.: 1972 *Proc. 3rd Lunar Sci.*, Lunar Science Institute, Houston, to be published.

Kaula, W. M., Schubert, G., Sjogren, W. L., and Wollenhaupt, H. D.: 1972 *Proc. 3rd Lunar Sci. Conf.*, Lunar Science Institute, Houston, to be published.

Kraner, H. W., Schroeder, G. L., Davidson, G., and Carpenter, J. W.: 1966, *Science* **152**, 1235.

Mandel'shtam, S. L., Tindo, I. P., Chermemukhen, G. S., Sorokin, L. S., and Dimitriev, A. B.: 1968, 'Lunar X-rays and the Cosmic X-ray Background Measured by the Lunar Satellite', UDC 523:36 :629. 192.32 (translated from *Komisches. Isled.*, c, 119, (1968)).

Meyer, C., Jr.: 1972, *Proc. 3rd Lunar Sci. Conf.*, Lunar Science Institute, Houston, to be published.

Patterson, James H., Turkevich, Anthony L., Franzgrote, Ernest J., Economou, Thanasis E., and Sowinski, Ernest P.: 1972, *Science*, **168**, 825.

Reedy, R. C., Arnold, J. R., and Trombka, J. I.: 1972, submitted to *J. Geophys. Res.*

Tucker, W. H., and Koren, M.: 1971, *Astrophys. J.* **168**, 283.
Van Dilla, M. A., Anderson, E. C., Metzger, A. E., and Schuch, R. L.: 1962, *Ire Transact. Nucl. Sci.* **NS-9**, No. 3.
Vinogradov, A. P., Surkov, Yu, A., Chernov, G. M., Kirnozov, F. F., and Nazarkina, G. G., 1968, *Moon and Planets* II, 77.
Wood, J. A.: 1972, *Icarus* **16**, 462.
Whitaker, E. A.: 1965, in Hess, Menzel and O'Keefe (eds.), *The Nature of the Lunar Surface, The Surface of the Moon*, The Johns Hopkins Press, p. 79.